Effect of climate change on the land rent of radiata pine plantations in Chile: Site productivity and forest fires

Rodrigo Labbé [a], Mario Niklitschek [b,*], Marco Contreras [b]

[a] *Universidad Austral de Chile, Faculty of Forest Sciences and Natural Resources, Graduate School, Campus Isla Teja, Valdivia, Chile*
[b] *Universidad Austral de Chile, Faculty of Forest Sciences and Natural Resources, Institute of Forest and Society, Campus Isla Teja, Valdivia, Chile*

ARTICLE INFO

ABSTRACT

Climate change can severely affect forest plantation productivity and fire regimes in temperate regions. The economic evaluation of these impacts is challenging because of the spatially differentiated effects expected to occur across planted areas. We calculated the combined effect of projected climate change on the stochastic land expectation value (SLEV) for a random sample of stands covering the *Pinus radiata* plantations in central-southern Chile. To simplify the stochastic evaluation problem with changing productivity and fire frequencies over time, we divided rotations into stages, before and after commercial thinning, and assumed that reforestation is at the end of each stage. The SLEV was calculated through Monte Carlo simulations using the coefficients from previously estimated productivity and fire risk statistical models. The predicted combined effect on the SLEV is negative in most regions except those in the southern limit of the specie distribution. In the economically crucial coastal area of the central regions, the negative effect of more frequent fires outweighs faster growth. In the northern drier areas, the SLEV becomes negative due to a large drop in site productivity. Anticipatory reassignments of management regimes have a large adaptation value in these low-productivity sites. Our optimization-simulation results suggest that relative to prescribed management regimes, the optimal rotation age in most low-productivity sites is longer and in most high-productivity sites shorter. Shortening the rotation age by one to two years has an important adaptation value in highly productive coastal sites.

1. Introduction

Radiata pine plantations in Chile covers approximately 1.5 million ha or 60% of the total forest plantation area. The climate is Mediterranean temperate and humid, with yearly precipitations from 500 to 2000 mm and a dry season extending from zero months in the southern limit of the planted distribution to eight months in low latitudes of the eastern side of the coastal range. The northern planted areas were severely affected after 2010 by droughts and large fires, causing the burning of more than 285 thousand ha in the 2016–2017 fire season (Garreaud et al., 2020). More recently, forest fires affected more humid and lower temperature areas further south, damaging 230 thousand ha in the 2022–2023 fire season. These higher latitude areas, where most of the more productive radiata pine plantation forests are located, have experienced a trend toward lower precipitation and higher temperature (Dirección Meteorológica de Chile, 2018; 2019).

The management has evolved from producing pulp and low-quality saw-timber in the 80s to producing clear timber (knot-free) in high-productivity sites since the mid-90s (Meneses and Guzman, 2000). Innovations that facilitated the change in management included developing new genotypes, improving plant production technology to reduce mortality, and intensifying plantation establishment using additional pre and post-planting weed control treatments, subsoiling, and fertilization (Burdon et al., 2017). The most intensive management regime to produce clear timber involves a non-commercial and one commercial thinning, three pruning, and rotation ages 22 to 24 years (Meneses and Guzman, 2000). This intensification of forest production and specialized regimes according to site productivity provides the landowner management options for adapting to the observed and projected effects caused by climate change within the bounds of historical and geographic variability. However, forest management adaptation based primarily on on-site productivity changes might be suboptimal because it ignores the projected changes in fire risk. For example, in coastal areas, adopting more intensive management regimes with longer rotations in response to projected higher productivity might not be efficient, resulting in a lower land forest because of more frequent and intense fires. The rising

---

projected temperatures that would increase productivity would also cause higher inflammability, larger fuel load, and more frequent fires (Niklitschek and Labbé, 2023).

As in other temperate regions, the response to the observed higher fire activity has focused on strengthening fire suppression capacity, resulting in substantial increases in investment and operational costs, reaching an annual budget in 2020–2021 fire session of 170 million dollars considering public and private expenditures. However, preventive forest management is still mainly limited to building fire breaks and other vegetation treatments along stripes around the urban-forest interface (CONAF, 2017).

Estimating the economic effect of climate change and identifying appropriate site-specific adaptation measures requires assembling high-spatial-resolution data. For example, Hannah et al. (2011) and Guo and Costello (2013) addressed the variability in California forest productivity to analyze specie substitution and changes in rotation age under climate change scenarios using a 1/8° resolution grid (about 16.000 ha). They found a high adaptation value by substituting *Tsuga heterophylla* (Raf.) stands located in the southern limit of the specie distribution with *Sequoia sempervirens* (D. Don), a specie better adapted to higher temperatures and able to produce more valuable timber. However, this adaptation measure was appropriate only for a relatively small forest area along the coast. Adjustments in the rotation age were more broadly applicable but had a low adaptation value. Their dynamic optimization, however, did not consider the effect of climate change on fire risk.

Unlike the substantial research efforts on mapping fire risk under climate change at different scales (Amatulli et al., 2013; Bedia et al., 2015; Parks et al., 2016), the economic analysis considering fire risk and high spatial resolution data is limited. A recent exception is Mei et al. (2019), who studied the entry and exit decisions of forest landowners facing uncertain revenues from price and climate-induced fires at the county level in the southeastern United States. The net effect of climate change due to higher growth and higher timber revenue volatility results in lower entry and exit thresholds, implying a higher probability of new planting areas and a lower probability of abandoning forest land. Therefore, the net impact of climate change on the planted area would be positive. In their real options analysis, fire frequency over rotations is constant and management adaptation measures including changes in the rotation age are not considered.

Previously, Stollery (2005) extended Reed's (1984) classical formulation to analyze the optimal rotation age under a positive trend in fire risk resulting from climate change. His simulation exercise used parameters of typical single stands of three species of Canadian boreal forests. In his forward-looking anticipatory formulation, the land expectation value (LEV) was calculated as the expected present value of the stumpage value of subsequent rotations considering an increasing fire probability. Unlike Reed's formulation, he breaks from the Faustmann's tradition of constant flows and infinite rotations. Stollery's simulation results indicate that anticipating a higher fire frequency in future rotations reduces the optimal rotation age of the current rotation. Therefore, following a myopic strategy by updating Reed's rotation age with a constant fire risk in future rotation yields a rotation age that is longer than optimal.

Other contributions after Reed (1984) kept the assumption of constant fire risk over rotations but considered more flexible management options. A relevant theoretical result is that the shortening effect of fire risk on the optimal rotation age persists if a fraction of the timber volume is salvaged (Amacher et al., 2005; Hyytiäinen and Haight, 2010; Ferreira et al., 2014). Another interesting result is that by choosing a management regime with a lower planting density, the landowner can mitigate financial losses from fire risk, reducing the rotation age less severely (Amacher et al., 2005; Hyytiäinen and Haight, 2010). More surprisingly, Amacher et al. (2005), in their simulation exercise for a loblolly pine site, found that the optimal rotation age under fire risk could be higher than the deterministic solution if plantation density and fuel treatment options are available. Similarly, using optimal control,

Patto and Rosa (2022) extended the Reed formulation to consider the joint optimization of continuous commercial thinning and the rotation age. They found that by anticipating commercial thinning, the fire-caused losses on the standing stock decline, avoiding the shortening of the rotation age. Daigneault et al. (2010) and Ferreira et al. (2014), using discrete stochastic dynamic optimization, found for a given plantation density, lower optimal rotation age under fire risk even when adjustments in intermediate fuel treatment interventions are considered (thinning and understory removal). None of these studies analyze the optimal rotation age under a fire risk that increases in future rotations due to changing climate conditions.

This article seeks to answer the following research questions: What is the impact of climate change on the stochastic land expectation value (SLEV) of radiata pine plantations across its geographic distribution in Chile, considering the combined effect on productivity and forest fires? Are there areas that could cease to be economically viable because of climate change? What is the financial benefit for the landowner to reassign management regimes according to projected site productivity? What is the landowner's value in optimizing the rotation age under the new conditions of site productivity and fire risk? To answer these questions, we calculated the SLEV for a random sample of polygons equal to or smaller than 25 ha covering the radiata pine plantations in central-southern Chile. The SLEV of each polygon was obtained through Monte Carlo simulations using an evaluation spreadsheet implemented with parameters estimated previously in productivity and fire risk statistical models. We follow an anticipatory strategy similar to Hyytiäinen and Haight (2010) to obtain near-optimal rotation ages in subsequent rotations for a subsample of randomly selected polygons.

2. Data

2.1. Sample design

The study covers the area of radiata pine plantations from the Maule administrative region in the north to Los Lagos region in the south (34° to 42° south latitude). Each region was subdivided from west to east to consider longitudinal climate variation due to the effect of the coast and the Andes mountain ranges, using the classification of Schlatter and Gerding (1995) (Fig. 1).

Our sampling units were polygons that resulted from the intersection of a 500 m climate grid and the latest update (made between 2013 and 2016, depending on the region) of the radiata pine cover completed at the regional level by the Forest National Corporation (CONAF for its acronym in Spanish).[1] A sample was randomly selected for each sub-region using the National Simulation Model Center (MNS)[2] growth zones as a stratum. In addition to climate variability, the MNS zones represent different soil characteristics. This sampling strategy provided a manageable database for the stochastic simulation at the polygon-stand level. Table 1 shows the number of polygons, the areas in the population and sample, the average stumpage value under both current and first-period projected climate (2021–2045).

Using the stumpage value as the interest variable, our sample size of 5122 polygons has a 2% error for each subregion at a significance level of 0.01. The stumpage value was obtained using the volume projections of the Insigne simulator of the MNS based on the site index (SI) and management regime. The SI for radiata pine represents the average height of the dominant and codominant trees at the age of 20 years (Gavilán-Acuña et al., 2021). The source of management, harvest and transportation cost and log prices and the mill are described in the product prices and management costs section.

The variance calculation considered unequal area among sampling

---

[1] https://www.conaf.cl/nuestros-bosques/bosques-en-chile/catastro-vegetacional/

[2] https://www.mnssimulacion.cl/
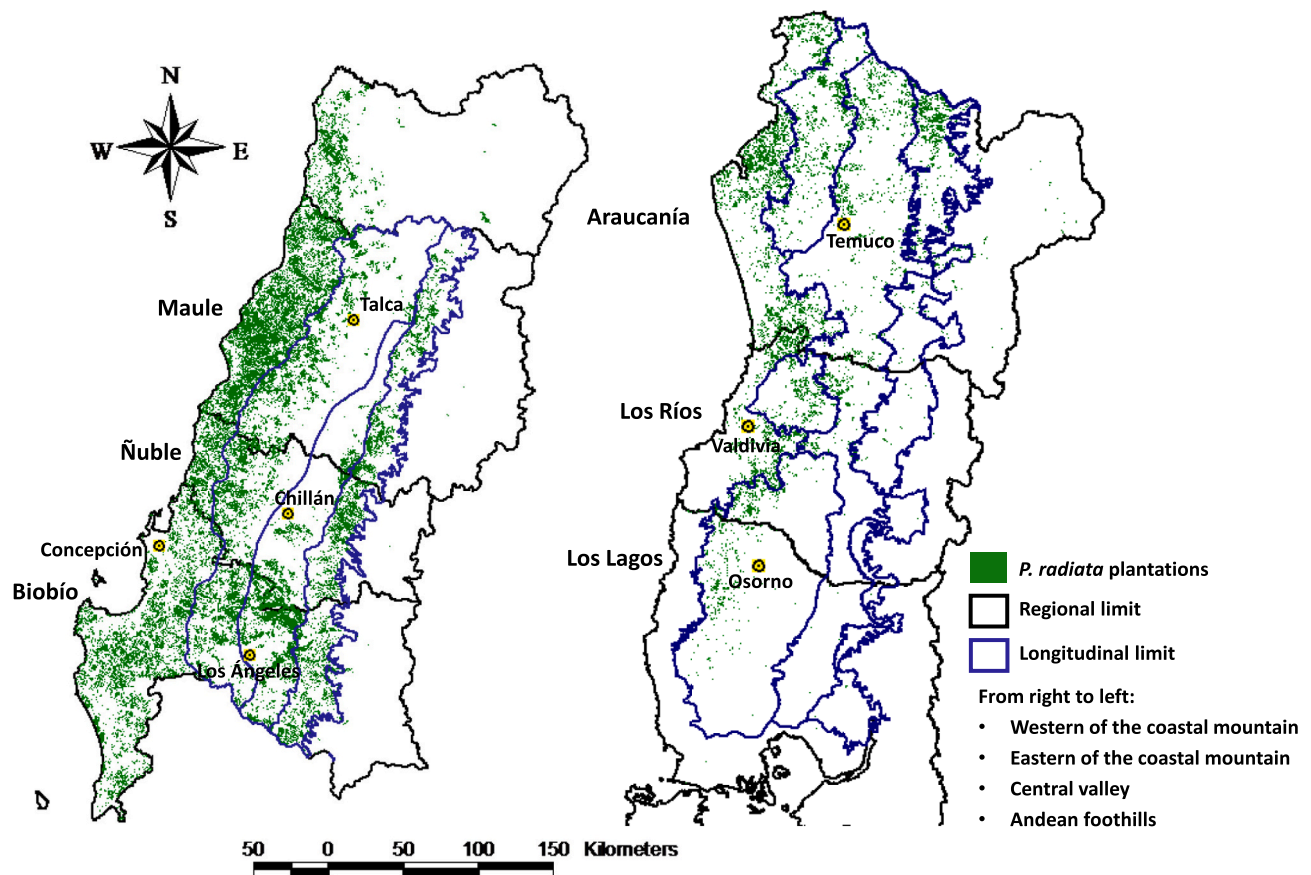
Fig. 1. The distribution of radiata pine plantations in Chile by administrative regions and longitudinal zones following the classification of Schlatter and Gerding (1995).

Table 1
Population parameters and sample size.

Region or subregion	Number of polygons	Plantation area (ha)	Number of strata	Stumpage 1990–2010 (USD ha^{-1})	Stumpage 2021–2045 (USD ha^{-1})	Polygons in the sample	Sample area (ha)
Maule	**21,693**	**471,493.3**		**10,934.1**	**10,068.2**	**1665**	**36,684.5**
Coast	12,664	278,907.2	2	11,891.8	11,391.8	256	5725.4
Eastern side	5508	122,621.8	2	7787.1	6428.2	1000	22,483.4
Central valley	586	13,038.5	1	9489.4	7882.4	172	3820.7
Andean foothills	2935	56,925.8	1	12,996.5	11,625.9	237	4655.2
Ñuble	**10,377**	**231,155.9**		**12,104.7**	**11,151.8**	**948**	**21,549.7**
Coast	2520	54,917.5	2	14,050.6	14,080.0	129	2808.0
Eastern side	3343	75,964.3	3	9708.2	8414.1	392	8830.2
Central valley	2036	48,502.1	3	10,012.9	8281.2	302	7251.8
Andean foothills	2478	51,772.0	1	15,078.8	14,227.1	125	2659.7
Biobío	**20,633**	**450,935.0**		**14,129.4**	**13,617.6**	**1666**	**38,525.2**
Coast	10,498	219,822.8	2	16,658.8	17,098.8	335	7146.8
Eastern side	3565	82,829.2	2	9690.6	7914.1	462	10,935.9
Central valley	3752	89,331.2	2	10,360.0	8334.1	710	17,061.7
Andean foothills	2818	58,951.9	2	15,344.7	14,902.4	159	3380.9
Araucanía	**11,029**	**228,618.9**		**14,558.8**	**15,234.1**	**461**	**9394.0**
Coast	4935	97,977.9	4	14,375.3	15,642.4	300	5939.9
Eastern side	2022	45,236.7	2	13,650.6	13,436.5	66	1442.6
Central valley	2384	51,065.0	3	15,070.6	15,025.9	35	773.1
Andean foothills	1688	34,339.2	1	15,461.2	16,569.4	60	1238.3
Los Ríos	**4415**	**81,630.4**		**16,117.6**	**17,114.1**	**329**	**6266.8**
Coast	1977	35,703.1	2	15,829.4	17,049.4	92	1663.6
Eastern side	1662	31,021.7	2	16,360.0	17,155.3	127	2432.1
Central valley	666	13,014.4	1	16,247.1	17,002.4	89	1777.7
Andean foothills	110	1891.3	1	16,828.2	17,707.1	21	393.5
Los Lagos	**925**	**17,635.7**		**15,594.1**	**17,170.6**	**53**	**1009.5**
Coast	32	431.8	1	16,975.3	18,551.8	0	0.0
Eastern side	861	16,622.8	1	15,578.8	17,170.6	45	855.2
Central valley	20	379.2	1	15,350.6	16,512.9	7	139.1
Andean foothills	12	201.9	1	13,438.8	14,642.4	1	15.2
Total	**69,072**	**1,481,469.2**	**41**	**13,037.6**	**12,662.4**	**5122**	**113,430**

units, which resulted from the intersection of the climatic 500 m grid and the radiata pine plantation cover (e.g. Niklitschek and Trincado, 2011). We selected the largest variation coefficient between the one calculated using data for the reference period (1990–2010) and the one with the first projected period (2021–2045) under RCP 8.5 climate change scenario. The sample allocation to each stratum was proportional to the stratum's population area.

2.2. Climate and timber volume

We use monthly temperature and precipitation data at a 500-m resolution generated by a team of climate scientists using statistical downscaling techniques which is described by Carrasco (2021). In our simulations under future climate conditions, the projections of the HadGEM2-ES global circulation model were used because they fall in the middle range of 29 models analyzed (Carrasco, 2021). This model projections have also been used to study the climate change effect on radiata pine plantations in Australia and New Zealand (Ivković et al., 2016). We assessed intermediate and pessimistic emission scenarios using the RCP 4.5 and RCP 8.5 (Taylor et al., 2012). For the scenario without climate change, we replicated the data from the reference period (1990–2010) to complete the two projected periods, 2021–2045 and 2046–2070.

A critical input for our analysis was volume projections for the site indexes (SI), and management regimes of our sample units. We predicted the SI for the reference period (1990–2010) and two projected periods (2021–2045 and 2046–2070) under the two climate change scenarios, using the empirical model implemented in the Insigne simulator of the MNS. Each simulation yields harvest volumes for each product at different rotation ages and management regimes.

To reflect prevailing management practice, six different management regimes were allocated according to the sampling unit SI. As shown in Table S1 in the appendix, the management regimes included three intensive regimes for units with SI greater than 26.5, two extensive management regimes for intermediate productivity units and for units with an SI less than 19.5 a pulp regime without commercial thinning a pruning.

The annual fire probability under current and future climate was obtained using the parameters of a previously estimated panel data model. Both the model specification and partial effect estimates are in Niklitschek and Labbé (2023). For each polygon in our sample, the probability was projected annually for 2021–2070, keeping constant non-climate covariates except for the stand age and the SI. Climate covariates affect the probability of stand ignition directly and indirectly through their effect on the stand productivity (SI). The fire probability varies with the calendar year and the stand age.

The data used in our damage cost calculations came from post-fire inventories and price and cost records of one of the largest forest companies in Chile. The post-fire inventory covers 26,450 ha of *P. radiata* burned during 2016–2021. This burned area was classified into three categories of damage intensity: (i) Low damage associated with surface fires, (ii) moderate damage associated with passive crown fires, and (iii) severe damage associated with active crown fires.[3] In the moderate and severe categories were 80% of the affected area, which needed to be harvested and reforested post-fires, according to the company's practice. According to the post-fire inventories, the percentage of the commercial volume loss for young and mature stands were 20.3 and 6.4%, respectively. In addition, for the same period the market prices of the damaged wood sold by the company were penalized by 5.8% for clear wood, 9.0% for sawn wood, and 23.7% for pulp wood. Approximately 50% of the total harvested volume in burned areas were damaged. The cost of post-fire reforestation has been 350 USD ha^{-1} and 550 USD ha^{-1} higher in

young and mature stands than an unburned stands, respectively. This higher cost is required to clear and crush the remanent burned trees.

2.3. Product prices and management costs

The costs of silvicultural interventions vary among management regimes, as shown in table S1 in the appendix. The plantation cost depends on the quality of plants, planting density, fertilizer application, and the number of weed control treatments. Pruning cost increases with pruning height and the number of pruned trees. The cost of non-commercial thinning increases with the number of trees removed.

Transportation costs vary by product type. For clear and sawn logs, we calculated the average transportation distance between the centroid of each subregion and the three closest sawmills with an annual production greater than 5000 m^3. For pulpwood, we used the distance to the nearest pulp mill. The location data of industrial facilities (updated to 2020) was downloaded from the CONAF information site.[4] Transport distances were calculated with the Bing Maps Truck Routing API application and assuming minimum time routes. Harvest cost is sensitive to mean volume per tree, reflecting the lower harvest productivity in stands with small-diameter trees. Table S2 in the appendix presents the harvest and transportation cost estimates and prices by product type.

3. Evaluation model

3.1. Determining the impact of climate change on the stochastic LEV and the value of reassigning management regimes

The analysis of the optimal rotation age under fire risk typically assumes that the fire frequency and site productivity are constant over rotations (Reed, 1984; Amacher et al., 2005; Susaeta et al., 2016). To analyze the effect of climate change, however, we needed to follow a more flexible specification differentiating the flows of benefits and costs over rotations. Using the generalized Faustmann formulation proposed by Chang (1998, 2020), we introduced differences in productivity and fire frequency for the period with climate data projections, affecting the financial flows of the first two or three rotations. A similar approach, although ignoring fire risk, was used to determine the value of forest management adaptation in California (Hannah et al., 2011; Guo and Costello, 2013).

To reduce the complexity of the stochastic evaluation problem associated with the large number of possible fire trajectories involved in using annual fire events, we divided the rotation into two stages, before and after commercial thinning. For the pulp management regime which does not have commercial thinning, our first stage for young forest end at year nine. This is half of the rotation age according to the prescribed management. As in Hyytiäinen and Haight (2010), and Ferreira et al. (2014) we assume that post-fire reforestation occurs at the end of each stage. Fig. 2 shows the possible fire trajectories of a stand planted in 2021 during the period with climate data projections (2021–2070). The stand can reach four possible states at the end of a stage indicated by the superscript in each node: young stand without fire (1), young stand with fire (2), a mature stand without fire (3), and mature stand with fire (4). If the state of the stand is young without fire in the fourth stage, there is a fifth stage to complete the rotation. There are 21 possible fire trajectories: 2^4 possible realizations at the end of stage four plus five trajectories resulting from adding a fifth stage to those trajectories ending in a young, unburned stand.

The stochastic LEV ($E(LEV)_k$) for a stand k is obtained as:
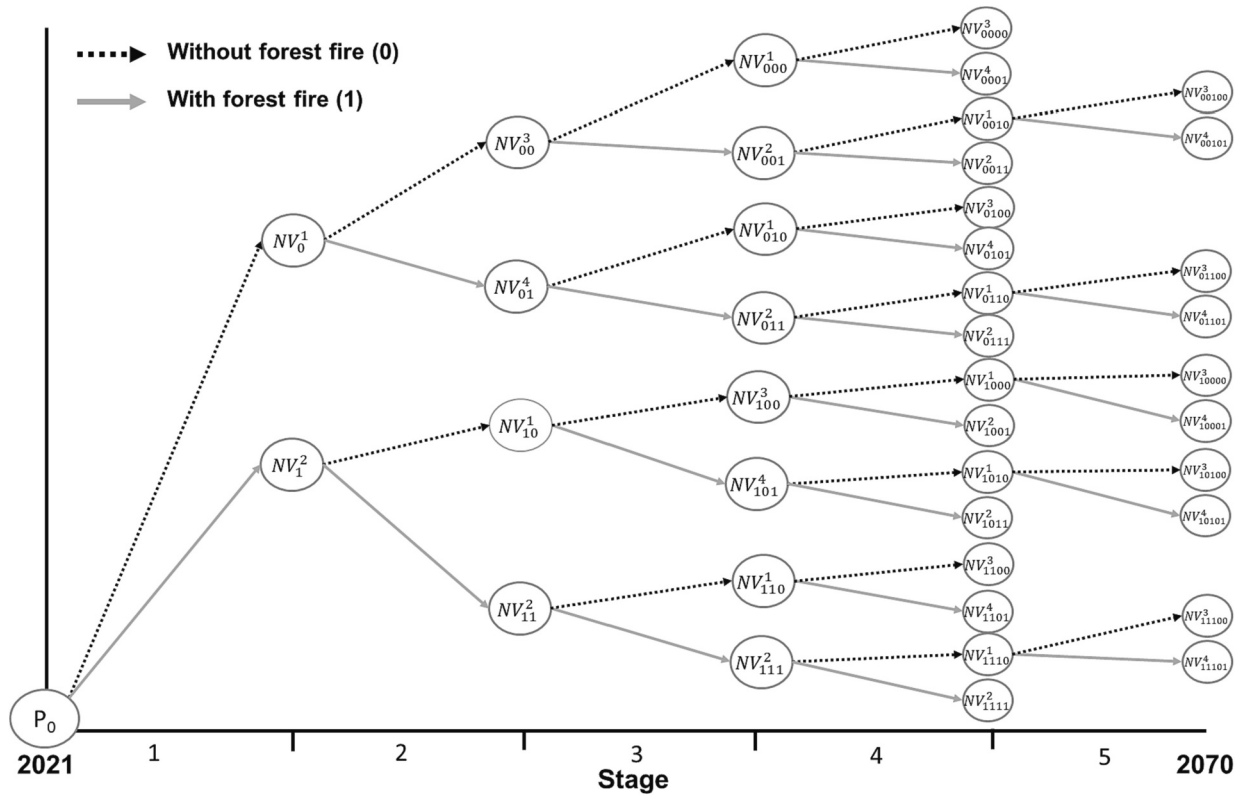
Fig. 2. Tree of fire trajectories. Each node is characterized by the net value (*NV*) of the stage. The subscript denotes the firing trajectory previous to each node, where zero indicates no fire and one fire. The superscript indicates the state of the forest at the end of the stage: young stand without fire (1), young stand with fire (2), mature stand without fire (3), and mature stand with fire (4).

$$E(LEV)_k = -C_0 + \sum_{i=1}^{m} \sum_{j=1}^{n_i} \left(pr_{(j|i)} NV_{ij} (1+r)^{-\sum_{l=1}^{j} t_{il}} \right) + LEV_R (1+r)^{-\sum_{l=1}^{n_i} t_{il}} + \frac{C_a}{r} \tag{1}$$

Where i denotes the fire trajectory and j the stage. The number of trajectories is denoted by m, and the number of stages by n_i. The number of stages required to complete a rotation or end with a burn stand can be four or five, depending on the fire trajectory, as shown in Fig. 2. The length of a stage is denoted by t_{il} and depends on the fire trajectory. If the stage corresponds to a young stand, it ends at commercial thinning, and if it is an adult stand because no fire existed in the previous stage, it lasts from commercial thinning to harvest. Both periods vary with the management scheme as indicated in Table S1.

The net value of a stage (NV_{ij}) is calculated as follows:

$$NV_{ij} = \begin{cases} TVY - PNC & \text{if young stand without fire} \\ SVY - PNC - RCY & \text{if young stand with fire} \\ TVM - RC & \text{if mature stand without fire} \\ SVM - RCM & \text{if mature stand with fire} \end{cases} \tag{2}$$

Where *TVY* denotes the net revenue from commercial thinning, *PNC* the costs of pruning and non-commercial thinning capitalized at the end of the stage, *SVY* the net revenue from salvaged wood of a young stand, *RCY* the reforestation cost of a young burned stand, *TVM* the net revenue of a mature stand or stumpage value, *RC* the reforestation cost of an unburned stand, *SVM* is the net revenue from salvage wood of a mature stand and *RCM* the reforestation cost of a burned mature stand.

We denote by $pr_{(j|i)}$ the probability of fire in stage j conditional on trajectory i. Similarly to the discrete time approach follow by Martell (1980) and Hyytiäinen and Haight (2010), we calculate this probability as:

$$pr_{(j|i)} = \frac{1}{m-1} \prod_{l=1}^{j} P(I_{il}) \tag{3}$$

$P(I_{ij})$ denotes the probability that a fire "*I*" occurs in the stage j of trajectory i. The probability that the stand is ignited is $P(I_{ij} = 1) = d_j$ and the probability that the fire does not occur is $P(I_{ij} = 0) = (1 - d_j)$. For example, the probability of fire in the third stage for the fire trajectory without an event in the first rotation and fire before commercial thinning in two consecutive stages ($j = 0011$ in Fig. 2) is $pr_{j=3\setminus i=0011} = \frac{(1-d_1)(1-d_2) d_{i3}}{20}$. It can be shown that $\sum_{i=1}^{21} \left(\sum_{j=1}^{4} pr_{(j|i_4)} + \sum_{j=1}^{5} pr_{(j|i_5)} \right) = 1$.

LEV_R denotes expected land value for infinite rotations calculated with the Reed (1984) generalization of the Faustmann formula under the presence of forest fires and partial timber damage. In the calculation of LEV_R, we use the stumpage value of the second rotation, the fire probability of the fourth or fifth stage and timber damage and reforestation cost of a mature stand. The discount rate and administrative costs are represented by r and C_a, respectively.

The rotation age affects wood volumes by product type, which is reflected in the stumpage value with and without fire (*TVM* and *SVM* in eq. 2). The stand ignition probability $P(I_{ij} = 1)$ is also affected by the stand age depending on the site productivity, as reflected by the conditional partial effects estimated in Niklitschek and Labbé (2023). The stand ignition probability increases monotonically with the stand age, but with a lower rate for more intensive management regimes. The effect of the rotation age on the stochastic LEV also depends on the discounting factor, as indicated in eq. 1.

The average stochastic LEV by subregion was obtained considering unequal polygon area sizes and sample stratification (Cochran, 1977, pp. 143–144) as follows:

$$E(LEV) = \frac{\sum_{h=1}^{H} \left(\frac{A_h}{a_h}\right) \sum_{k=1}^{n} E(LEV)_k a_k}{\sum_{h=1}^{H} \left(\frac{A_h}{a_h}\right) a_h} \qquad (4)$$

Where a_k is the area of polygon k, a_h is the sample area and A_h is the total area with radiata pine plantations in stratum h. Assuming independence among polygons, we can also obtain the standard error (*SE*) by subregion by replacing in eq. 4 the average polygon values with the standard errors that resulted from the Monte Carlo simulations.

We considered three scenarios of alternative management regimes under current and projected climate conditions:

$\gamma_1 =$ current management regimes under current climate conditions.

$\gamma_2 =$ current management regimes under projected climate (business as usual).

$\gamma_3 =$ reassigned management regimes under projected climate (adaptation).

The adaptative value of reassigning management regimes corresponds to $E(LEV)_{\gamma_3} - E(LEV)_{\gamma_2}$, and assuming that the forest landowner adapts or reassigns the management regime to the projected productivity, the economic impact of climate change to $E(LEV)_{\gamma_3} - E(LEV)_{\gamma_1}$.

We used the following values: (i) $r = 0.08$ (ii) $C_a = 25.4$ USD and iii) an exchange rate of 1 USD to 850 CLP (Central Bank of Chile, December 31, 2021).

3.2. Determining the value of adapting the rotation age

We use an optimization-simulation procedure to calculate a near-optimal rotation age (Fig. 3). This approach combines an optimization procedure that estimates the optimal value of the decision variables and a stochastic simulation model that estimates the expected value of the objective function (Glover et al., 2000). This stochastic optimization approach has been used in the analysis of forest management decisions under fire risk by González et al. (2005) in the northeast of Spain and Hyytiäinen and Haight (2010) in the northwestern United States. The procedure parameters were set at one thousand simulations and one thousand iterations for each simulation.

Due to the processing time required, we carried out this analysis in one randomly selected polygon for each subregion and stratum instead of the entire sample and considering only the most pessimistic climate change scenario (RCP 8.5). The spatial distribution of the 29 selected polygons is shown in Fig. S1 of the appendix.

To calculate the value of the optimal rotation age relative to the current company prescription and adapting it to climate change, we defined three scenarios under the current management regime (business as usual), and one with reassigned management regime:

$\gamma_4 =$ without climate change and the rotation age optimized under the current climate.

$\gamma_5 =$ with climate change and the rotation age optimized under the current climate.

$\gamma_6 =$ with climate change and the rotation age optimized under projected climate.

$\gamma_7 =$ with climate change and the rotation age optimized under projected climate but using the reassigned management regime.

Thus, we calculated the value of the optimal rotation age as:

i) $E(LEV)_{\gamma_4} - E(LEV)_{\gamma_1}$, without climate change.
ii) $E(LEV)_{\gamma_6} - E(LEV)_{\gamma_2}$, with climate change and maintaining the current management regime (business as usual).
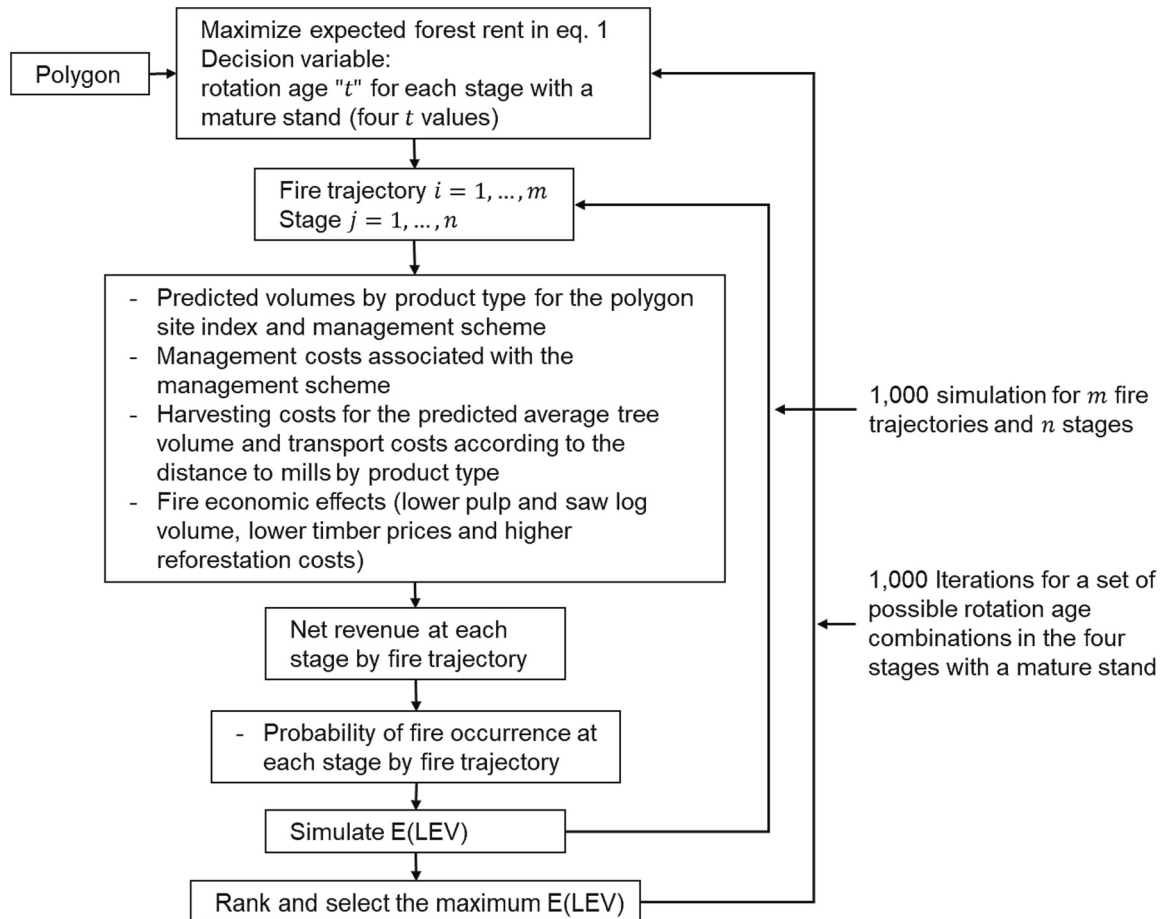
Fig. 3. Illustration of the optimization-simulation procedure.

iii) $E(LEV)_{\gamma_7} - E(LEV)_{\gamma_3}$, with climate change and reassigning the management regime.

And the adaptative value was calculated as $E(LEV)_{\gamma_6} - E(LEV)_{\gamma_5}$.

We used the Crystal Ball Oracle risk analysis software to implement the Monte Carlo simulations for sample polygons and the optimization-simulation procedure for sub-sample polygons (Glover et al., 2000).

4. Results

4.1. The effect of climate change on the expected LEV

Table 2 show the differences on the stochastic LEV under projected climate conditions relative to current climate and considering the two scenarios of alternative management regimes. Table two also show the adaptative value of reassigning management regimes. The values of stochastic LEV under current and projected climate can be reviewed in table S3 of the appendix. The impact of climate change on the average stochastic LEV is negative for all subregions north of the Araucanía. The largest absolute decline is observed in the eastern side (497.3 USD ha^{-1} for the RCP 4.5 and 748.7 USD ha^{-1} for the RCP 8.5) and central valley (508.5 and 752.4 USD ha^{-1}, respectively) of Biobío region (Table 2, column 4 for RCP 4.5 and column 6 for RCP 8.5). These differences would be greater if forest landowners do not reassign the management regimes according to the projected site productivity (Table 2, column 3 for RCP 4.5 and column 5 for RCP 8,5).

The Araucanía would also experience a reduction in the stochastic LEV, with more severe effects projected for the eastern hill side of the coastal range due to the projected decrease in site productivity. However, the changes would be smaller in the coast and the stochastic LEV would even increase in the foothills of the Andes Mountain range under the RCP 8.5 (Table 2). The regions south of the Araucanía would

experience an increase in the stochastic LEV as a result of a higher site productivity and a fire probability that remain at a low level.

The regions of Maule and Ñuble, located in the north of the specie distribution, would be severely affected. Under both climate change scenarios, the eastern hillside of these regions would have a negative stochastic LEV (table S3 in appendix). Under the RCP 8.5, the coast of Ñuble would also face this unfavorable state. From the approximately 1.5 million ha currently planted, 198 and 266 thousand hectares would cease to be attractive to be reforested with radiata pine in these regions under the RCP 4.5 and RCP 8.5, respectively.

4.2. The adaptive value of reassigning forest management regimes

We calculated the value of reassigning management regimes in response to projected productivity by comparing the average stochastic LEV of the reassigned management regime with the business as usual. Column 7 in Table 2 provides the result for the RCP 4.5 and column 8 for the RCP 8.5. The adaptive value of reassigning management regimes is higher in those subregions where the impact of climate change on the average forest is larger. For example, for the central valley of Biobío region reached a difference of 249 and 363 USD ha^{-1} under the RCP 4.5 and RCP 8.5, respectively. This subregion is characterized by sandy soils with low water retention capacity and low productivity (Schlatter and Gerding, 1999). Conversely, the lowest adaptive values are in the coast and fluctuates for the three regions in a range of 51 to 106 USD ha^{-1} and 83 to 197 USD ha^{-1} under both climate scenarios, respectively.

Site productivity decline resulting from projected climate change north of Araucanía would cause a large increase in the proportion of the radiata pine plantation area assigned to extensive and pulp forest management regime (Fig. 4). These changes in the management regime would occur mainly in the eastern hillside on the coastal range and in the central valley. For the Andean foothills of northern regions, the

Table 2

Projected impact of climate change on the stochastic LEV ($E(LEV)$) and the adaptative value of reassigning management regimes in radiata pine plantations under fire risk.

Region	Planted area (ha)	Impact of climate change (RCP 4.5) (USD ha^{-1})		Impact of climate change (RCP 8.5) (USD ha^{-1})		Adaptative value of reassigned management regime (USD ha^{-1})	
		Business as usual	With reassignment	Business as usual	With reassignment	RCP 4.5	RCP 8.5
(1)	(2)	(3)	(4)	(5)	(6)	(7)	(8)
Maule	**471,493**	**−398.9**	**−290.8**	**−645.2**	**−467.7**	**108.1**	**177.5**
Coast	278,907	−347.7	−278.6	−574.3	−461.3	69.1	113.0
Eastern side	122,621	−458.3	−304.0	−715.4	−459.6	154.3	255.8
Central valley	13,038	−635.4	−425.8	−993.7	−553.5	209.6	440.2
Andean foothills	56,925	−468.0	−291.4	−761.7	−497.7	176.6	264.0
Ñuble	**231,155**	**−560.1**	**−438.5**	**−892.0**	**−686.7**	**121.6**	**205.3**
Coast	54,917	−510.4	−459.5	−864.1	−780.7	50.9	83.4
Eastern side	75,964	−593.0	−433.3	−930.9	−650.4	159.7	280.5
Central valley	48,502	−708.8	−565.8	−1027.5	−788.5	143.0	239.0
Andean foothills	51,772	−425.4	−304.7	−737.8	−544.9	120.7	192.9
Biobío	**450,935**	**−502.0**	**−355.9**	**−828.4**	**−590.6**	**146.1**	**237.8**
Coast	219,822	−384.6	−278.7	−714.4	−517.5	105.9	196.9
Eastern side	82,829	−656.4	−497.3	−1001.8	−748.7	159.1	253.1
Central valley	89,331	−757.0	−508.5	−1115.2	−752.4	248.5	362.8
Andean foothills	58,952	−335.1	−212.9	−573.8	−394.7	122.2	179.1
Araucanía	**228,619**	**−266.7**	**−239.0**	**−311.2**	**−271.7**	**27.7**	**39.5**
Coast	97,978	−131.0	−142.2	−155.8	−174.0	−11.2	−18.2
Eastern side	45,237	−520.2	−423.3	−704.0	−585.5	96.9	118.5
Central valley	51,065	−458.3	−369.4	−511.5	−376.6	88.9	134.9
Andean foothills	34,339	−39.0	−81.4	56.2	15.5	−42.4	−40.7
Los Ríos	**81,630**	**14.3**	**37.5**	**155.7**	**170.2**	**23.2**	**14.5**
Coast	35,703	38.8	72.1	204.4	226.5	33.3	22.1
Eastern side	31,022	−9.5	24.2	110.6	141.5	33.7	30.9
Central valley	13,014	−2.9	−29.2	124.6	80.7	−26.3	−43.9
Andean foothills	1891	62.9	63.3	189.4	190.8	0.4	1.4
Los Lagos	**17,636**	**185.2**	**174.8**	**370.6**	**385.3**	**−10.4**	**14.7**
Eastern side	16,623	186.6	175.9	375.1	390.3	−10.7	15.2
Central valley	379	159.8	159.8	280.7	280.7	0.0	0.0
Andean foothills	202	118.5	118.5	198.8	198.8	0.0	0.0
Total	**1,481,469**	**−406.1**	**−302.7**	**−633.1**	**−464.9**	**103.4**	**168.2**
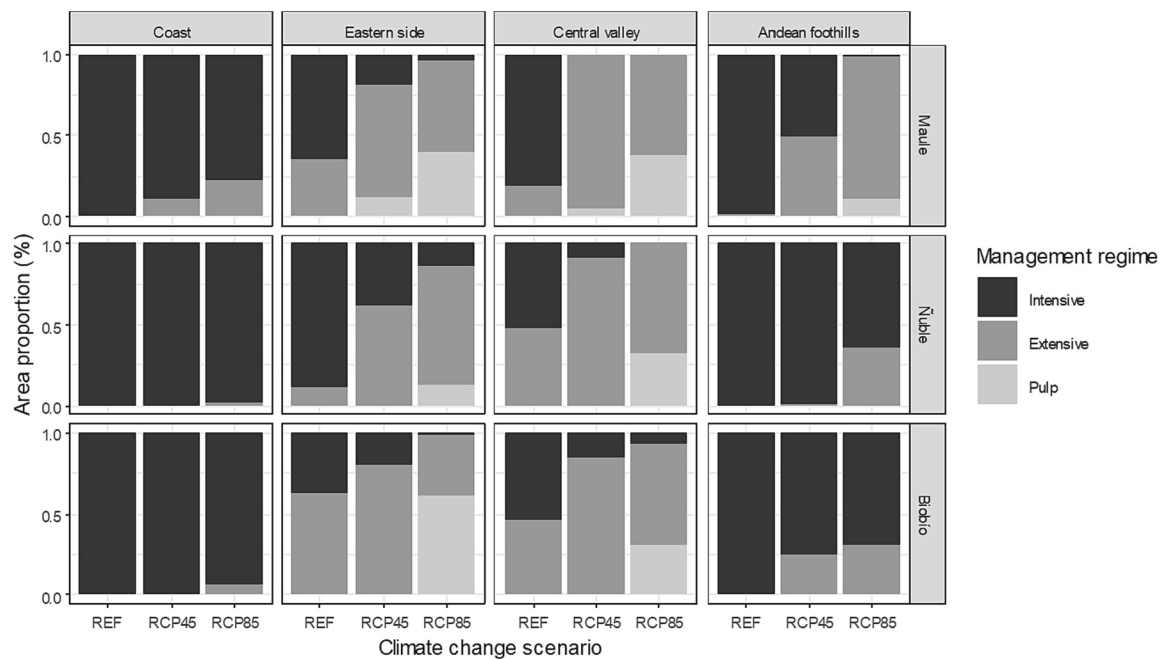
Fig. 4. Proportion of the *P. radiata* plantation area by management regime considering the current climate (REF) and the RCP 4.5 and RCP 8.5 scenarios for 2046–2070.

reassignment from the intensive to the extensive management regimes would also be important. The cost saving from the exclusion of non-commercial thinning and pruning resulted in a higher average stochastic LEV in these areas affected by an important reduction on site productivity. The lower proportion of plantation area managed intensively would drop the availability of saw timber and clear timber for the forest industry in these regions.

The adaptive values for the southern regions (Araucanía and south of the Araucanía) was lower or negative, between −42 to 97 USD ha^{-1} and -44 to 135 USD ha^{-1} under the RCP 4.5 and RCP 8.5, respectively (Table 2). For these subregions the stochastic LEV remained high or experienced moderate increases.

Table 3
Location, site index (SI) and annual fire probability of occurrence in polygons randomly selected for the optimization-simulation procedure.

Polygon	Region	Zone	Current climate		Climate change RCP 8.5 scenario			
					2021–2045		2046–2070	
			SI (m)	Annual probability*	SI (m)	Annual probability*	SI (m)	Annual probability*
1	Maule	Coast	30.7	0.0387	30.3	0.0673	28.1	0.0929
2	Maule	Coast	31.5	0.0249	31.3	0.0403	29.4	0.0640
3	Maule	Eastern side	28.2	0.0375	26.9	0.0470	22.0	0.0353
4	Maule	Eastern side	22.8	0.0051	20.5	0.0058	12.2	0.0003
5	Maule	Central valley	28.0	0.0265	26.5	0.0605	20.4	0.0321
6	Maule	Central valley	28.5	0.0097	26.9	0.0222	20.4	0.0104
7	Maule	Andean foothills	28.1	0.0090	26.7	0.0240	20.6	0.0114
8	Ñuble	Coast	31.4	0.0299	31.1	0.0562	29.2	0.0738
9	Ñuble	Eastern side	28.4	0.0262	27.0	0.0543	22.6	0.0416
10	Ñuble	Eastern side	29.0	0.0319	27.8	0.0691	23.8	0.0608
11	Ñuble	Central valley	24.8	0.0051	23.2	0.0107	17.8	0.0031
12	Ñuble	Andean foothills	32.5	0.0093	31.8	0.0256	27.9	0.0387
13	Biobío	Coast	33.9	0.0080	34.0	0.0177	33.0	0.0298
14	Biobío	Coast	30.5	0.0504	29.8	0.1121	27.0	0.1388
15	Biobío	Eastern side	29.9	0.0308	28.9	0.0676	25.5	0.0756
16	Biobío	Eastern side	24.6	0.0119	22.9	0.0191	17.8	0.0066
17	Biobío	Central valley	25.1	0.0083	23.6	0.0151	18.6	0.0057
18	Biobío	Central valley	26.5	0.0078	25.2	0.0162	20.5	0.0084
19	Biobío	Central valley	30.4	0.0128	29.4	0.0291	25.2	0.0331
20	Biobío	Andean foothills	28.1	0.0037	27.3	0.0103	23.5	0.0095
21	Araucanía	Coast	31.5	0.0019	32.2	0.0075	32.0	0.0159
22	Araucanía	Coast	29.6	0.0080	30.7	0.0230	31.3	0.0466
23	Araucanía	Eastern side	30.9	0.0266	30.6	0.0625	28.8	0.0707
24	Araucanía	Central valley	33.5	0.0041	33.5	0.0083	32.0	0.0163
25	Araucanía	Andean foothills	32.0	0.0011	33.0	0.0026	33.0	0.0070
26	Los Ríos	Coast	30.3	0.0134	31.5	0.0009	32.1	0.0011
27	Los Ríos	Eastern side	31.5	0.0088	32.1	0.0096	31.7	0.0195
28	Los Ríos	Central valley	32.5	0.0005	33.4	0.0012	33.4	0.0014
29	Los Lagos	Eastern side	30.1	0.0000	31.3	0.0000	32.1	0.0000

4.3. The optimal adaptation of the rotation age

In our subsample (Table 3), the polygons with the lowest SI were located north of the Araucanía in the eastern hillside of the coastal range (polygons 3, 4, 9, 10, 15 and 16), the central valley (polygons 5, 6, 11, 17, 18 and 19) and the Andean foothills (polygons 7, 12 and 20). On the other hand, the highest SI polygons are located from the Araucanía region to the south (polygons 21 to 29) and in the coast from Maule to Biobío (polygons 1, 2, 8, 13 and 14). The SI and the annual fire frequency in Table 3 represent the average values over a full rotation and under the RCP 8.5. In our simulations, the annual fire frequency, in addition to the SI, depended on stand age, which varied with the fire trajectory, and the calendar year.

(*) The annual probability is calculated using prescribed rotation ages according to the stand site index.

The procedure described in Fig. 2 maximizes the stochastic LEV, as specified in eq. 1, using the rotation age of the mature stand as the control variable. Depending on the fire trajectory, the harvest can occur in any stage between stages two to five, and thus fourth control variables are needed. In the deterministic case, the harvest happens in stages two and four to complete the first two rotations. The maximum number of iterations was set at 1000 and 300 if achieved no improvements in the objective function value. The processing time varied depending on the fire frequency, with almost three hours for high fire probability polygons in the north and less than 15 min for a low fire frequency polygon in the south. In all cases, the optimal solution was achieved before the one-thousand iteration limit.

As expected, the optimal rotation age under fire risk was equal to or less than the deterministic optimal rotation age (table S4 of the appendix). Four of the 29 polygons analyzed experienced a reduction of the stochastic optimal rotation age under the current climate and 13 with the projected climate under the RCP 8.5 scenario. Without climate change, the decrease in the rotation age can reach two years, and with climate change as many as five years.

We compared our results under the current and climate change RCP 8.5 scenarios with the values in prescribed management regimes (Table 4). Columns 2 to 5 show the difference between the optimal and the prescribed rotation age in the four stages under the current climate. For low productivity sites, the optimal rotation age is the same as the prescribed one (polygons 4, 5, 6, 9, 10), one year (polygons 3, 11, and 18), or two years longer (polygon 17). Conversely, for high-productivity sites (polygons 1, 2, 8, 13, 14, and 19 to 29) the optimal rotation age is several years shorter, ranging from one to six years.

Columns 7 to 10 show the same differences but under the RCP 8.5 scenario and without reassigning management regimes. For low-productivity sites, the difference increased, reaching a maximum of four years in polygons 4 and 18. If management regimes are reassigned according to projected site productivity (columns 12 to 15), the difference increases to six or seven years. This large increase in the optimal rotation age occurs in those polygons where the extensive saw timber regime is replaced by a pulpwood regime (polygons 4, 11, 16, and 17). For high-productivity sites, the results under climate change are similar to those under the current climate.

The optimal adaptation of the rotation age, maintaining the other prescribed interventions unchanged, is shown in Columns 17 to 20. Table 3 shows that the optimal rotation age increased with climate change in most polygons located north of the Araucania where productivity is projected to decline. Longer rotations are observed even in polygons that would suffer a significant increase in the fire probability (polygons 1, 8, 14, and 15). However, if site productivity remained high, as in polygons 2 and 13, a higher fire probability was associated with a reduced optimal rotation age.

In five of the nine polygons in the Araucanía region and further south, the optimal adaptation is to shorten the rotation age (polygons 21, 22, 25, 26, and 28). These polygons would experience either a rise in productivity, a rise in forest fire activity, or both. The value of adapting

the rotation age is higher in these more productive sites reaching 228 USD ha^{-1} in polygon 19.

S: stage at which the mature forest is harvested.

5. Discussion and conclusions

In this article, we analyze the impact of climate change on the stochastic land expectation value (stochastic LEV), considering changes in site productivity and fire probability for a sample of polygons covering the *P. radiata* plantation area in central and southern Chile. Our sample of 5122 polygons reflects the climate and soil variability across the area of the specie distribution and most differences in transportation and harvest costs. We calculate the stochastic LEV under current and future climate, with and without adaptation of management regimes to projected productivity changes. As a measure of site productivity, the SI is used by forest companies to differentiate management regimes, allocating the production of high-value timber to the best sites. Therefore, the reassignment of management regimes according to the SI projected changes seems to be a natural response and anticipatory adaptive measure more likely to be implemented by landowners. We also explore the value of adapting the rotation age for a subsample of sites in response to projected productivity and fire activity changes.

The stochastic LEV is substantially lower than the deterministic LEV for current climate and fire frequency, which is consistent with the results obtained in previous studies (Reed, 1984; Patto and Rosa, 2022). Under projected climate conditions, the relative economic importance of fire substantially increases in most of the radiata pine area distribution in Chile.

The impact of climate change on the stochastic LEV depends on the initial climate conditions. In non-coastal areas of the northern regions of the specie distribution, the projected temperature increase and precipitation decline from unfavorable levels would result in a substantial drop in site productivity and stochastic LEV. The lower fuel availability would constrain the fire frequency in these zones despite the more favorable climate conditions for its flammability. More than 200 thousand hectares would become economically unattractive for forest production despite the reassignment to extensive pulp management. This management regime adjustment would significantly reduce the availability of high-value timber in these low productivity areas.

The stochastic LEV would also decline in the coastal areas of these northern regions. Unlike non-coastal sites, however, the negative effect of climate change is caused by increased fire frequency that results from greater flammability, while the site productivity changes only slightly. The low changes in site productivity reduce the opportunity for reassigning existing prescribed management regimes. Measures oriented to reduce the frequency of stand ignition and to increase the timber salvage value, such as fuel treatment and earlier and more intense thinning, might have a high adaptation value.

The central region of the specie distribution (the Araucanía) would also experience a reduction of the stochastic LEV in a magnitude similar to the coast of the northern regions. This region has more favorable initial climate conditions with higher precipitation, less extreme temperatures during the growing season, and lower productivity differences between the coast and non-coastal areas. This region would experience a significant increase in the frequency of fire and moderate changes in site productivity.

The stochastic LEV would increase under the projected climate change in the more humid and colder southern regions due to higher site productivity resulting from the increase in temperature and a low fire frequency. Our results show that reassigning management regimes according to the projected higher productivity would have a low or negative adaptive value. This suggests the need to develop new management regimes for these high-productivity sites, modifying the intensity and timing of thinning and pruning interventions.

We found important differences between the rotation age of currently applied management regimes and our optimization results.

Table 4

Differences in the optimal rotation age with and without climate change and the value of adaptation.

Polygon	Value of optimizing																Value of adaption				
	Under current climate					Business as usual					Reassigned										
	S2	S3	S4	S5	USD ha^{-1}	S2	S3	S4	S5	USD ha^{-1}	S2	S3	S4	S5	USD ha^{-1}	S2	S3	S4	S5	USD ha^{-1}
(1)	(2)	(3)	(4)	(5)	(6)	(7)	(8)	(9)	(10)	(11)	(12)	(13)	(14)	(15)	(16)	(17)	(18)	(19)	(20)	(21)
1	−3	−3	−3	−3	308.1	−3	−2	−2	−2	219.5	−2	−1	−1	−1	225.3	0	1	1	1	22.2
2	−4	−1	−4	−4	168.2	−4	−4	−4	−1	129.0	−4	−3	−3	0	105.3	0	−3	0	3	12.2
3	1	1	−1	1	21.3	1	1	1	1	27.0	1	2	0	2	18.3	0	0	2	0	10.8
4	0	0	0	0	9.7	2	4	4	4	68.7	5	7	7	7	117.3	2	4	4	4	68.7
5	0	0	0	0	0	1	0	−2	1	57.0	2	−1	−1	4	59.2	1	0	−2	1	57.0
6	0	0	0	0	7.1	0	1	1	1	34.4	1	3	2	2	37.3	0	1	1	1	34.4
7	0	0	0	0	11.3	1	0	0	0	68.4	2	1	−2	1	68.7	1	0	0	0	68.4
8	−4	−4	−4	−4	303.6	−3	−2	−2	−2	158.7	−3	−1	−1	−1	140.1	1	2	2	2	69.3
9	0	0	0	0	13.9	1	1	1	1	30.7	2	2	2	2	32.9	1	1	1	1	30.7
10	0	0	0	0	48.9	1	1	−1	3	37.3	1	0	0	3	38.8	1	1	−1	3	37.3
11	1	1	1	1	164.4	2	2	2	2	95.5	3	6	6	6	108.6	1	1	1	1	53.1
12	−4	−4	−4	−4	629.9	−4	−3	−3	−3	380.4	−3	−1	−1	−1	403.6	0	1	1	1	42.1
13	−5	−5	−5	−5	1097.1	−7	−6	−6	−6	982.0	−7	−6	−6	−6	982.0	−2	−1	−1	−1	117.1
14	−3	−3	−3	−3	208.8	−2	0	0	0	47.7	−1	1	1	−2	43.0	1	3	3	3	12.8
15	−2	−2	−2	−2	252.6	−1	1	−2	1	128.4	−3	−1	−1	2	4.9	1	3	0	3	49.1
16	−1	−1	−4	−1	94.2	−3	2	−1	2	19.5	−2	6	6	6	32.6	−2	3	3	3	21.9
17	1	1	−2	1	137.4	−1	3	3	3	36.5	0	7	7	7	55.6	−2	2	5	2	78.5
18	1	0	1	1	51.2	3	4	4	4	131.1	4	−1	−1	−1	105.4	2	4	3	3	30.8
19	−3	−3	−3	−3	314.1	−2	−2	−2	−2	242.1	−1	−1	−1	−1	111.9	1	1	1	1	227.9
20	−1	−1	−1	−1	58.6	0	3	−1	3	23.3	0	4	0	4	24.4	1	4	0	4	99.8
21	−3	−3	−3	−3	467.6	−4	−4	−5	−4	559.8	−4	−4	−5	−4	559.8	−1	−1	−2	−1	164.5
22	−2	−2	−2	−2	221.1	−1	−1	−4	−1	169.9	−1	−1	−4	−1	169.9	1	1	−2	1	67.2
23	−3	−3	−3	−3	240.1	−3	−1	−2	−1	187.9	−2	−1	−2	−1	152.2	0	2	1	2	18.0
24	−5	−5	−5	−5	762.4	−5	−4	−4	−4	718.9	−4	−4	−4	−4	702.1	0	1	1	1	21.7
25	−3	−3	−3	−3	446.2	−4	−4	−4	−4	550.3	−5	−5	−5	−5	612.1	−1	−1	−1	−1	184.9
26	−3	−3	−5	−3	372.2	−5	−4	−5	−5	554.1	−5	0	−5	−5	554.1	−2	−1	0	−2	81.5
27	−5	−5	−5	−5	506.4	−5	−4	−4	−4	669.9	−5	−4	−4	−4	668.8	0	1	1	1	50.1
28	−6	−6	−6	−6	777.8	−7	−7	−7	−7	928.0	−7	−7	−7	−7	928.0	−1	−1	−1	−1	74.5
29	−4	−4	−4	−4	254.6	−4	−4	−4	−4	447.1	−4	−4	−4	−3	447.1	0	0	0	0	0.0

The largest potential financial gains are found by shortening the rotation age in high-productivity sites under the current and projected climate. According to our results, delaying harvest to increase the participation of high value knot-free timber in the total stumpage value is not profitable. However, the market prices in our analysis might not be sufficiently differentiated by quality and reflect the shadow prices for vertically integrated companies. Furthermore, the cost of log segregation might require a minimal volume of high-value logs in the harvested stand. However, our results suggest that the landowner's stochastic LEV is highly responsive to the rotation age for high-productivity sites. Further work determining the segregation cost and price differentiation according to the product specifications (log diameter and length) would provide a more conclusive result.

Our results suggest that considering the effect of climate change on fire frequency is important in the analysis of the adaptation value of the rotation age. For polygons located in the coast where a large increase in fire frequency is projected while productivity remains high, the average value of adapting the rotation age is 5.7% of the expected LEV with climate change. Previous studies that have only considered the effect on productivity have found rotation age adaptation values of less than 1% (Hannah et al., 2011; Guo and Costello, 2013).

Our estimation of the expected LEV assumes that climate change does not affect timber prices. The Chilean Forest industry is integrated into international markets, and long-term trends in local prices are likely to follow world market prices closely. The results of world market dynamic models have found lower prices by the end of the century (Sohngen and Tian, 2016). There is important uncertainty, however, particularly on the magnitude of CO_2 fertilization effect assumed in underlying growth process models and the management response. In a recent study of the U.S., despite the important impact on regional output, the effect on market prices is relatively small (Baker et al., 2022). Considering that our focus is on finding regional differences and implications for management adaptation, our assumption appears adequate. Because of our long-term and spatially detailed focus, it also seems reasonable to ignore the temporary effect of catastrophic fires on log prices.

A limitation of our analysis of the economic impact of climate change at the stand level is that the abandonment option after a fire is not considered. This is because the landowner might decide not to reforest a burned stand even if the anticipated stochastic LEV is positive because of the higher reforestation cost. With the abandonment option, the negative impact of climate change on the LEV would be lower because the expected future rent after a fire could not be negative. Likewise, it would increase the area allocated to other land uses.

Our result finds that reassigning management regimes according to the projected productivity increases the stochastic LEV in most subregions. Further work should consider variations in plantation density and the timing and intensity of thinning jointly with the rotation age. A stochastic dynamic programming formulation should include the abandonment option after a fire as in Ferreira et al. (2014). This optimization modeling effort needs to be complemented by improving the modeling of the fire frequency and making damage intensity sensible to forest management.

Authors' contributions

Rodrigo Labbé carried out the literature review, data analysis, drafted and edited the manuscript. Mario Niklitschek carried out the literature review, drafted, and edited the manuscript. Marco Contreras contributed to edit the manuscript and generated MNS volume simulation data.

Declaration of Competing Interest

The authors declare no competing financial interest.

Data availability

Data will be made available on request.

Appendix A. Supplementary data

Supplementary data to this article can be found online at https://doi.org/10.1016/j.forpol.2023.103068.

References

Amacher, G.S., Malik, A.S., Haight, R.G., 2005. Not getting burned: the importance of fire prevention in Forest management. Land Econ. 81 (2), 284–302. https://doi.org/10.3368/le.81.2.284.

Amatulli, Giuseppe, Camia, Andrea, San-Miguel-Ayanz, Jesús, 2013. Estimating future burned areas under changing climate in the EU-Mediterranean countries. Sci. Total Environ. 450-451, 209–222. https://doi.org/10.1016/j.scitotenv.2013.02.014.

Baker, Justin S., van Houtven, George, Phelan, Jennifer, Latta, Gregory, Clark, Christopher M., Austin, Kemen G., et al., 2022. Projecting U.S. forest management, market, and carbon sequestration responses to a high-impact climate scenario. Forest Policy Econ. 147, 1–17. https://doi.org/10.1016/j.forpol.2022.102898.

Bedia, Joaquín, Herrera, Sixto, Gutiérrez, Jose Manuel, Benali, Akli, Brands, Swen, Mota, Bernardo, Moreno, Jose Manuel, 2015. Global patterns in the sensitivity of burned area to fire-weather: implications for climate change. Agric. For. Meteorol. 214-215, 369–379. https://doi.org/10.1016/j.agrformet.2015.09.002.

Burdon, R.D., Libby, W.J., Brown, A.G., 2017. A wild ride, 1998 onwards. In: Burdon, Rowland D., Libby, W.J., Brown, A.G. (Eds.), Domestication of Radiata pine. springer (forestry sciences, 0924-5480, 83), Cham, Switzerland, pp. 335–396.

Carrasco, Gonzalo, 2021. High temporal and spatial resolution of bioclimatic variables on Central Chile for different climate change scenarios and global circulation models. Figshare. https://doi.org/10.6084/m9.figshare.14748471.v1.

Chang, Sun Joseph, 1998. A generalized Faustmann model for the determination of optimal harvest age. In *Can. J. For. Res.* 28 (5), 652–659. https://doi.org/10.1139/x98-017.

Chang, Sun Joseph, 2020. Twenty one years after the publication of the generalized Faustmann formula. For. Pol. Econom. 118, 102238. https://doi.org/10.1016/j.forpol.2020.102238.

Cochran, William G., 1977. Sampling Techniques, 3rd ed. Wiley (Wiley series in probability and mathematical statistics), New York, London.

CONAF, 2017. Protocolo de Plantaciones Forestales. Consejo de Política Forestal. Corporación Nacional Forestal (CONAF), Santiago, Chile. Available online at. https://www.conaf.cl/wp-content/files_mf/1511383027SegundoInformeProtocoloPlantaciones13Julio.pdf.

Daigneault, A.J., Miranda, M.J., Sohngen, B., 2010. Optimal Forest management with carbon sequestration credits and endogenous fire risk. Land Econ. 86 (1), 155–172. https://doi.org/10.3368/le.86.1.155.

Dirección Meteorológica de Chile, 2018. Reporte anual de la evolución del clima en Chile. Informe climático del año 2017. In: With Assistance of Dirección General de Aeronáutica Civil. Available online at. https://www.researchgate.net/publication/334611305.

Dirección Meteorológica de Chile, 2019. Reporte anual de la evolución del clima en Chile. Informe climático del año 2018. In: With Assistance of Dirección General de Aeronáutica Civil. Available online at. https://www.researchgate.net/publication/334611305.

Ferreira, L., Constantino, M., Borges, J.G., 2014. A stochastic approach to optimize maritime pine (Pinus pinaster Ait.) stand management scheduling under fire risk. An application in Portugal. Ann Oper Res 219 (1), 359–377. https://doi.org/10.1007/s10479-011-0845-z.

Garreaud, René D., Boisier, Juan P., Rondanelli, Roberto, Montecinos, Aldo, Sepúlveda, Hector H., Veloso-Aguila, Daniel, 2020. The Central Chile mega drought (2010–2018): a climate dynamics perspective. Int. J. Climatol. 40 (1), 421–439. https://doi.org/10.1002/joc.6219.

Gavilán-Acuña, Gonzalo, Olmedo, Guillermo Federico, Mena-Quijada, Pablo, Guevara, Mario, Barría-Knopf, Beatriz, Watt, Michael S., 2021. Reducing the uncertainty of radiata pine site index maps using an spatial ensemble of machine learning models. Forests 12 (1), 77. https://doi.org/10.3390/f12010077.

Glover, Fred, Kelly, James, Laguna, Manuel, 2000. The OptQuest approach to Crystall Ball simulation optimization. University of Colorado, Graduate School of Business, Colorado, USA (Decisioneering). Available online at. https://leeds-faculty.colorado.edu/glover/.

González, José Ramón, Pukkala, Timo, Palahí, Marc, 2005. Optimising the management of Pinus sylvestris L. stand under risk of fire in Catalonia (north-east of Spain). Ann. For. Sci. 62 (6), 493–501. https://doi.org/10.1051/forest:2005054.

Guo, Christopher, Costello, Christopher, 2013. The value of adaption: climate change and timberland management. J. Environ. Econ. Manag. 65 (3), 452–468. https://doi.org/10.1016/j.jeem.2012.12.003.

Hannah, L., Costello, C., Guo, C., Ries, L., Kolstad, C., Panitz, D., Snider, N., 2011. The impact of climate change on California timberlands. Clim. Chang. 109 (S1), 429–443. https://doi.org/10.1007/s10584-011-0307-2.

Hyytiäinen, Kari, Haight, Robert G., 2010. Evaluation of forest management systems under risk of wildfire. Eur J Forest Res 129 (5), 909–919. https://doi.org/10.1007/s10342-009-0278-2.

Ivković, Miloš, Hamann, Andreas, Gapare, Washington J., Jovanovic, Tom, Yanchuk, Alvin, 2016. A framework for testing radiata pine under projected climate change in Australia and New Zealand. New For. 47 (2), 209–222. https://doi.org/10.1007/s11056-015-9510-8.

Martell, D.L., 1980. The optimal rotation of a flammable forest stand. Can. J. For. Res. 10 (1), 30–34. https://doi.org/10.1139/x80-006.

Mei, Bin, Wear, David N., Henderson, Jesse D., 2019. Timberland investment under both financial and biophysical risk. Land Econ. 95 (2), 279–291. https://doi.org/10.3368/le.95.2.279.

Meneses, Mario, Guzman, Sergio, 2000. Productividad y eficiencia en la producción forestal basada en las plantaciones de pino radiata. Bosque 21 (2), 3–11.

Niklitschek, Mario, Labbé, Rodrigo, 2023. Modeling stand fire probabilities with unobserved heterogeneity. Estimating partial effects of the stand age and climate change in Chilean radiata pine plantations. Unpublished results..

Niklitschek, Mario E., Trincado, Guillermo, 2011. A cost effective stratified two-stage sampling design to estimate the forest land area of southern Chile. Can. J. For. Res. 41 (7), 1509–1521. https://doi.org/10.1139/X11-040.

Parks, Sean A., Miller, Carol, Abatzoglou, John T., Holsinger, Lisa M., Parisien, Marc-André, Dobrowski, Solomon Z., 2016. How will climate change affect wildland fire severity in the western US? Environ. Res. Lett. 11 (3), 35002. https://doi.org/10.1088/1748-9326/11/3/035002.

Patto, João V., Rosa, Renato, 2022. Adapting to frequent fires: optimal forest management revisited. J. Environ. Econ. Manag. 111, 102570. https://doi.org/10.1016/j.jeem.2021.102570.

Reed, William J., 1984. The effects of the risk of fire on the optimal rotation of a forest. J. Environ. Econ. Manag. 11 (2), 180–190. https://doi.org/10.1016/0095-0696(84)90016-0.

Schlatter, Juan, Gerding, Victor, 1995. Método de clasificación de sitios para la producción forestal, ejemplo en Chile. Bosque 16 (2), 13–20. Available online at. http://mingaonline.uach.cl/scielo.php?script=sci_arttext&pid=S0717-92001995000200002&lng=es&nrm=iso>. ISSN 0717–9200.

Schlatter, Juan, Gerding, Victor, 1999. Productividad en el ejemplo de seis sitios característicos de la VIII Región con Pinus radiata D. Don. In *Bosque* 20 (1), 65–77. https://doi.org/10.4206/bosque.1999.v20n1-07.

Sohngen, Brent, Tian, Xiaohui, 2016. Global climate change impacts on forests and markets. Forest Policy Econ. 72, 18–26. https://doi.org/10.1016/j.forpol.2016.06.011.

Stollery, Kenneth, 2005. Climate change and optima rotation in a flammable forest. Nat. Resour. Model. 18 (1), 91–112. https://doi.org/10.1111/j.1939-7445.2005.tb00150.x.

Susaeta, Andres, Carter, Douglas R., Chang, Sun Joseph, Adams, Damian C., 2016. A generalized Reed model with application to wildfire risk in even-aged southern United States pine plantations. Forest Policy Econ. 67, 60–69. https://doi.org/10.1016/j.forpol.2016.03.009.

Taylor, Karl E., Stouffer, Ronald J., Meehl, Gerald A., 2012. An overview of CMIP5 and the experiment design. Bull. Amer. Meteor. Soc. 93 (4), 485–498. https://doi.org/10.1175/BAMS-D-11-00094.1.